ELSEVIER

European Journal of Pharmacology 360 (1998) 21–29

ejp

Mechanisms of bupivacaine action on Na^+ and K^+ channels in myelinated axons of *Xenopus laevis*

Johanna Nilsson, Fredrik Elinder, Peter Århem *

The Nobel Institute for Neurophysiology, Karolinska Institutet, S-171 77 Stockholm, Sweden
Department of Neuroscience, Karolinska Institutet, S-171 77 Stockholm, Sweden

Received 6 November 1997; revised 13 August 1998; accepted 21 August 1998

Abstract

The local anaesthetic bupivacaine has recently been proposed to inhibit Na^+ channels indirectly by making the resting potential less negative. To test this hypothesis we analysed the effects of bupivacaine on voltage and current clamped nodes of Ranvier. Contrary to the hypothesis, the leak current and the resting potential were unaffected. The Na^+ and K^+ channels were, however, affected at relatively low concentrations (33 μM). Steady-state activation curves were decreased without notable shift effects, whereas the Na^+ inactivation curve was decreased and shifted in negative direction. The effect on the Na^+ current was tentatively explained by a single-site, state-dependent binding model ($K_d = 44$ μM), while that on the K^+ current was explained by two population-specific mechanisms, one open-state dependent ($K_d = 550$ μM) and one state independent ($K_d = 59$ μM). The binding stoichiometry was higher than 1:1 for the main sites of action. In conclusion, bupivacaine exerts its main anaesthetic action on myelinated nerve axons by a direct modification of Na^+ channels.

Keywords: Bupivacaine; Myelinated axon; Na^+ channel; K^+ channel; Voltage clamp; Local anaesthetic

1. Introduction

Bupivacaine is an amide type local anaesthetic mainly used for surgical, obstetric, and acute and chronic pain therapy (see the work of Covino (1986)). Most local anaesthetics, including the amide type anaesthetics, are described as state dependent Na^+ channel pore blockers (Hille, 1977; Hondeghem and Katzung, 1977; Hille, 1992; for another opinion, see the work of Butterworth and Strichartz (1990)). However, to explain its differential effect on axons with varying diameter (Aδ and C axons are more blocked than Aα axons; see the work of Covino (1986)) bupivacaine has been proposed to inhibit Na channels indirectly by depolarising the membrane (Bräu et al., 1995). The proposal was based on the finding that bupivacaine specifically blocks voltage independent flickering K^+ channels, assumed to be essential for the resting potential (Koh et al., 1992). These channels are mainly found in thin myelinated axons, implying that these fibres are more sensitive to a bupivacaine block. However, these conclusions were based on patch-clamp experiments on axons that have been extensively treated by mechanical and enzymatic means, possibly affecting the channel properties. To test the hypothesis of indirect Na^+ channel effects under more physiological conditions we analysed the effects of bupivacaine on voltage clamped intact nodes of Ranvier.

No effect on the voltage-independent leak current or resting potential was found, not even at high concentrations (6 mM). In contrast, the voltage-dependent Na^+ and K^+ channels were affected at relatively low concentrations (33 μM). Like other local anaesthetics (see the works of Hille (1977) and Haydon et al. (1984)), bupivacaine caused a voltage-independent decrease of Na^+ and K^+ steady-state activation curves (no shift), whereas it caused a clearly voltage-dependent decrease of the steady-state Na^+ inactivation curve (a shift in negative direction). The results were explained in terms of modulated receptor mechanisms (Hille, 1977; Hondeghem and Katzung, 1977). In conclusion, bupivacaine exerts its anaesthetic action on myelinated axons mainly by a direct modification of Na^+ channels.

* Corresponding author. The Nobel Institute for Neurophysiology, Karolinska Institutet, S-171 77 Stockholm, Sweden. Tel.: +46-8-728-6903; Fax: +46-8-349-544; E-mail: peter.arhem@neuro.ki.se

0014-2999/98/$ - see front matter
PII: S0014-2999(98)00631-1

2. Materials and methods

2.1. Electrophysiology

Myelinated axons of different sizes were isolated from the sciatic nerve of unanaesthetized decapitated toads of the species *Xenopus laevis* as described by Frankenhaeuser (1957). The single axons were mounted in a recording chamber and cut at half-internode length on both sides of the node under investigation. In some experiments whole internodal lengths were used. The solution pools of the chamber were connected to a two-amplifier voltage-clamp system by KCl bridges (120 mM). The chamber design, amplifier circuitry, and balancing procedures were essentially the same as described by Dodge and Frankenhaeuser (1958), with some modifications described by Åhrem et al. (1973). The current was calculated from the recorded voltage at the output of the voltage-clamp amplifier, assuming an axoplasmic internodal resistance of 40 MΩ (see the work of Dodge and Frankenhaeuser (1958)). To improve the control of the membrane potential and to obtain good time resolution of the ion currents, the experiments were performed at relatively low temperature (8–10°C). (At higher temperatures the inherent frequency response limitations of the system could cause oscillatory responses. Furthermore, the capacity current is relatively slower compared to the ion currents than at lower temperatures and consequently complicates the separation of currents). Pulse generation and sampling were made using a TL-1 DMA interface (Labmaster, Axon Instruments, Foster City, CA) and the pCLAMP software (Axon Instruments). The pulse rate was 0.5 Hz and the sampling interval 20–100 μs.

2.2. Solutions

The test solution was applied to the pool with the node and consisted of bupivacaine HCl (Sigma, St. Louis, MO, USA) added to Ringer solution. This contained (in mM): NaCl 115.5, KCl 2.5, $CaCl_2$ 2.0, and Tris buffer (adjusted to pH 7.2) 5.0. The solution used in the end pools consisted of (in mM): KCl 120.0 and Tris buffer (pH 7.2) 5.0.

3. Results

3.1. No effect on leak current and resting potential

The first objective of the study was to investigate the role of the reported bupivacaine-sensitive flickering channels for the anaesthetic action by analysing effects of bupivacaine on the leak current. Since it has been reported that the bupivacaine sensitive channels occur more frequently in thin axons (Koh et al., 1992), we studied axons in a relatively broad size spectrum with diameters in the range from about 10 μm to about 20 μm. No effect was discovered (tested in 17 axons), not even at bupivacaine concentrations blocking 100% of the Na^+ and K^+ channel currents and at application times longer than 5 min.

These experiments were supplemented with experiments under current clamp conditions in which the effect of bupivacaine on the resting potential was investigated. In accordance with the findings above no effect was detected. Fig. 1 shows a typical recording of the resting potential during application of 6 mM bupivacaine. In summary, both the voltage and current clamp measurements suggest that bupivacaine does not act on myelinated axons by changing the resting potential and thereby inactivating Na^+ channels as proposed by Bräu et al. (1995).

3.2. Effects on Na^+ and K^+ channels

Contrary to the case of the leak current, bupivacaine clearly affected both Na^+ and K^+ currents. Fig. 2 shows the effect of 67 μM bupivacaine on a family of ion

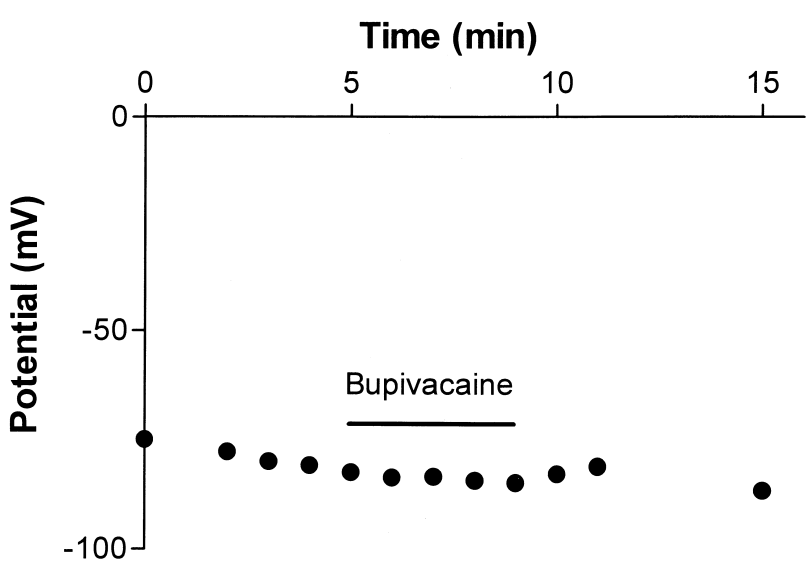

Fig. 1. Effect of bupivacaine on resting potential in control and in 6 mM bupivacaine solution (indicated by bar).

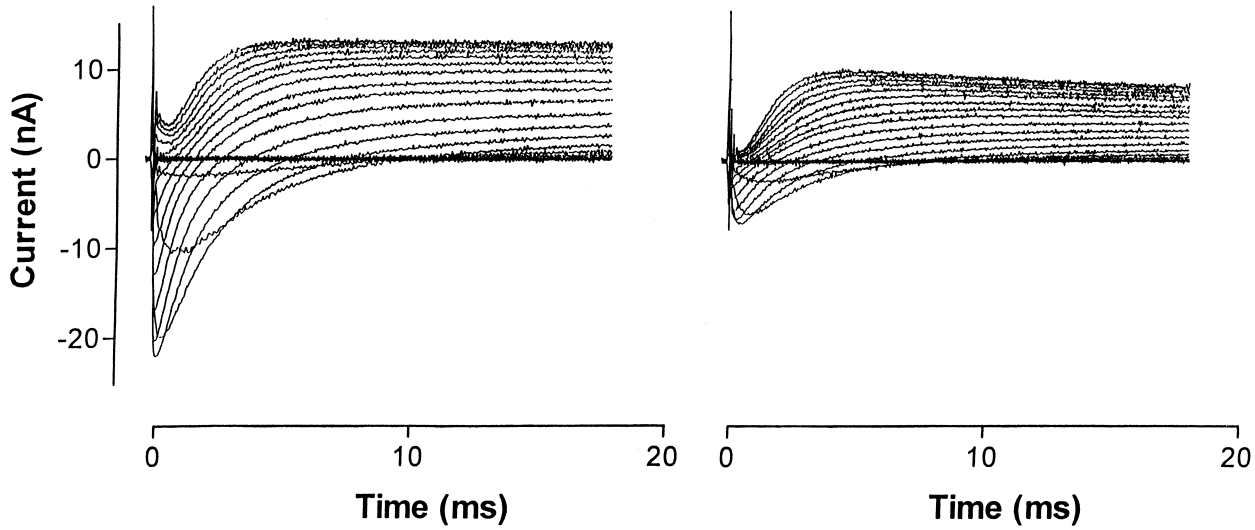

Fig. 2. Current families in control (left) and 67 μM bupivacaine (right). Potential steps in 10 mV increments from a holding potential of −90 mV. Leak current linearly subtracted.

currents associated with rectangular pulse steps. The transient Na^+ current was reduced by 70% with little or no change of time course. The delayed K^+ current was reduced by 30% and in contrast to the Na^+ current the reduction is associated with a time course change (i.e., with an induced inactivation). In the following we will analyse the results in terms of schematic binding models. Because of the variability of the response of each individual axon, concentration–response curves are presented for individual axons rather than as pooled data. This part of the investigation comprises data from 14 axons. For the detailed quantification presented below five of these were selected due to their stable responses over a wide range of concentrations.

3.2.1. Na^+ channels

Fig. 3A shows the peak Na^+ current plotted vs. potential at various bupivacaine concentrations in the range 33–100 μM. The bupivacaine-induced effect is mainly a general reduction or scaling of the current, independent of test step voltage, with 50 μM blocking 50% of the current. To investigate the effects on the steady-state inactivation we measured the peak Na^+ current at −10 mV from different prepulse potentials (duration 1 s). Fig. 3B shows results from such measurements, plotted as peak current vs. prepulse potential. The general reduction or scaling is here combined with a shift in negative direction. The effects were quantified by fitting the following Boltzmann function to the data:

$$I = I_{max} \Big/ \left(1 + \exp\left(\left(V - V_{1/2} - \Delta V_{1/2}\right)/s\right)\right). \quad (1)$$

The slope constant s and the midpoint potential $V_{1/2}$ (potential at 50% of max current) were obtained from fitting to control data. Fitting the curve to the bupivacaine data yielded a bupivacaine dependent scaling factor I_{max} and a bupivacaine dependent shift value $\Delta V_{1/2}$. In Fig. 3C the scaling factors I_{max} at different concentrations are plotted. A dose–response curve of the type

$$I_{max} = 1 \Big/ \left(1 + \left(c_{bup}/K_d\right)^{n_H}\right) \quad (2)$$

where c_{bup} is the the bupivacaine concentration, K_d the dissociation constant and n_H the Hill coefficient was fitted to the data. The mean (and SD) values for the five more extensively analysed (see above) axons were $K_d = 44 \pm 6$ μM and $n_H = 1.5 \pm 0.1$. The higher-than-one value of n_H suggests that at least two bupivacaine molecules bound to the same site are required to block the channel. Shift values for the same axon as in Fig. 3B are plotted in Fig. 3D.

The combined scaling and shift effects are possible to explain by a model assuming increased inactivation transition rates in bupivacaine bound channels. For the present results we used the following schematic model

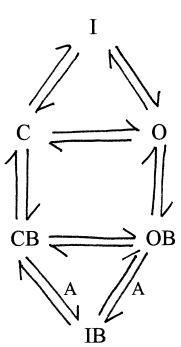

(3)

where C, O and I denote closed, open and inactivated states in unbound channels. CB, OB and IB denote the corresponding states in channels binding bupivacaine. An

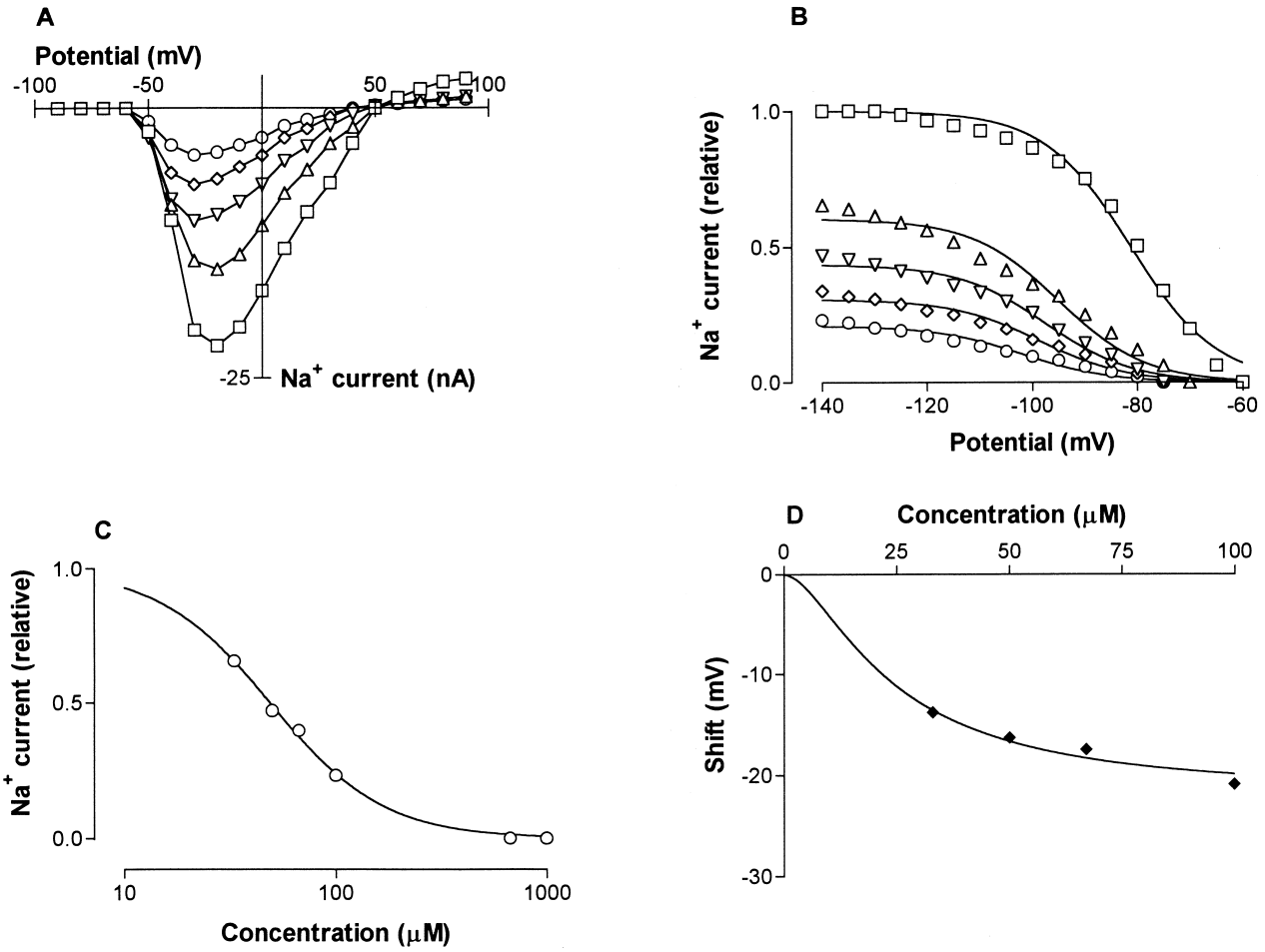

Fig. 3. Effect of bupivacaine on Na^+ channels. (A) Effect on the Na^+ peak current vs. voltage curve. (□) Control, (△) 33 μM, (▽) 50 μM, (◇) 67 μM and (○) 100 μM bupivacaine. (B) Effect on steady-state Na inactivation curve. Another axon than in (A) but same symbols. Continuous lines are solutions to Eq. (1). $s = -8.3$ mV and $V_{1/2} = -81$ mV. (C) Concentration dependence of scaling effect. Same axon as in (B). Continuous line is Eq. (2) fitted to the maximum steady-state inactivation values. $K_d = 49$ mV and $n_H = 1.6$. (D) Concentration dependence of shift effect. Same axon as in (B). Continuous line is Eq. (4) fitted to the shift of inactivation curve. $A = 13$ and $n_H = 1.9$.

increased rate of inactivation transitions in bound channels (CB → IB and OB → IB) is obtained by multiplying the corresponding rates in unbound channels (C → I and O → I) with the factor A. This scheme assumes that bupivacaine has access to the channel exclusively when it is in closed or open states to fit the results of other investigations presented in Section 4. The factor A can be determined from observed shift values $\Delta V_{1/2}$ according to the following relation derived in the Appendix A:

$$\Delta V_{1/2} = s \ln\left(1 + A\left(c_{bup}K_d\right)^{n_H}\right) \Big/ \left(1 + \left(c_{bup}K_d\right)^{n_H}\right) \qquad (4)$$

where s, K_d and n_H have the same meaning as in Eqs. (1) and (2). Fitting Eq. (4) to the shift data in Fig. 3D and using the values for s and K_d obtained from Fig. 3B and C ($s = -8.3$; $K_d = 49$ μM) yields $A = 13$ and $n_H = 1.9$. The mean (and SD) values of A and n_H for three fibres were 12 ± 2 and 1.9 ± 0.7, respectively. The shift data support the conclusion from the scaling data that the binding stoichiometry is higher than 1:1.

3.2.2. K^+ channels

Fig. 2 suggests that bupivacaine both causes a general time-independent and a time-dependent reduction of the K^+ current. To improve the resolution of the effect on the steady state current, especially important in the lower negative voltage range, we measured the effects on the instantaneous value of the current at a pulse step to +50 mV after 50 ms test steps. The measurements were made at a potential close to the Na^+ equilibrium potential, thus allowing measurements of K^+ currents uncontaminated by Na^+ current. Fig. 4A shows the open probability curves at various bupivacaine concentrations in the range 33–100 μM from such experiments. The main effect is clearly a general voltage-independent reduction of the curve (no shift), suggesting a relatively state independent block. The mean K_d of Eq. (2) fitted to the experimental data for the five axons was 69 ± 13 μM. (However, as will be discussed below, this value does not seem to reflect the affinity of a single binding site, but the mean affinity of a combination of two sites).

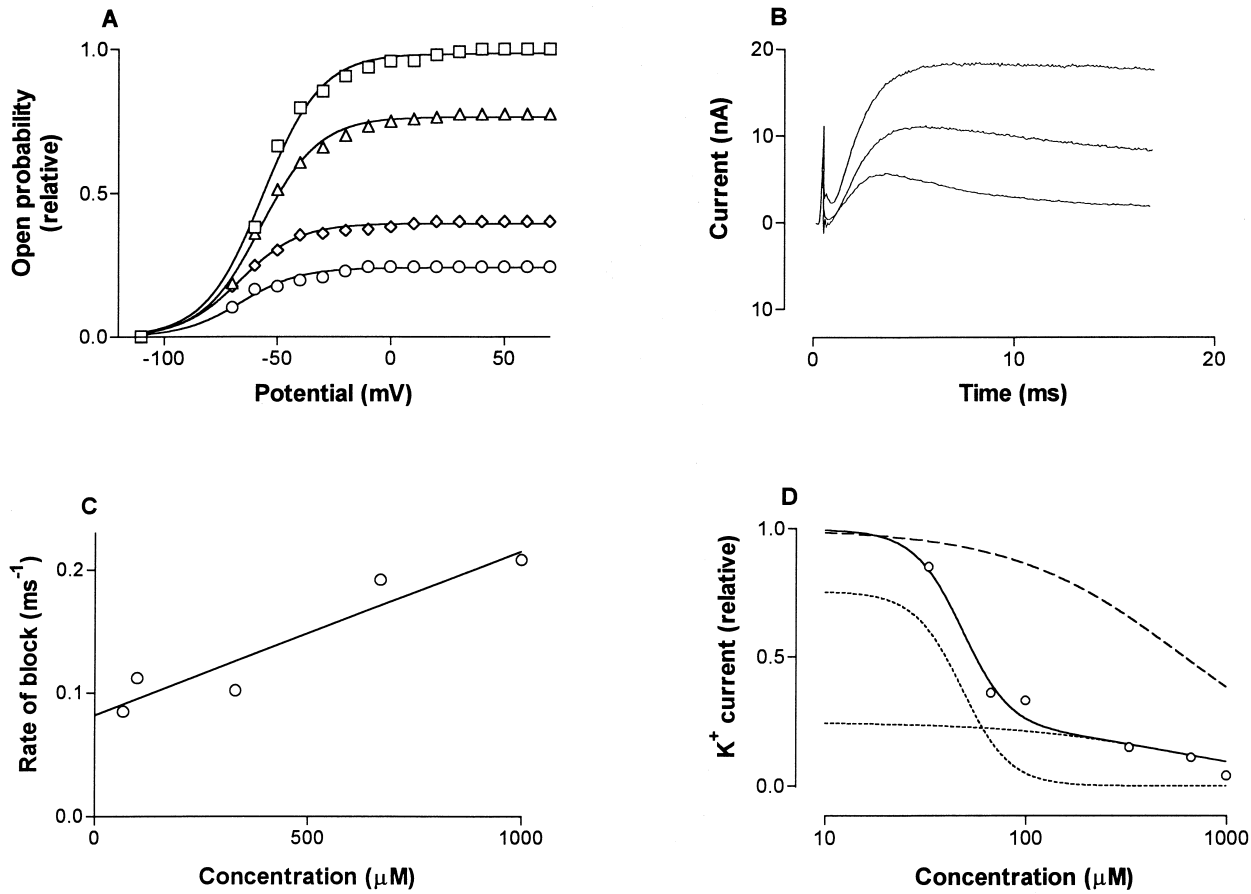

Fig. 4. Effect of bupivacaine on K^+ channels. (A) Open probability vs. voltage curve, measured as instantaneous value of tail current at +50 mV. (□) Control, (△) 33 μM, (◇) 67 μM and (○) 100 μM bupivacaine. Continuous lines are solutions to Eq. (1). (B) Bupivacaine induced K^+ current inactivation. Time course at +50 mV. Control (upper), 67 μM (middle) and 670 μM (lower) bupivacaine. (C) Concentration dependence of the rate of inactivation (inversed time constant). Continuous line is Eq. (5) fitted to data from axon in (B). $\lambda = 0.08$ ms^{-1} and $\kappa = 0.13$ ms^{-1} mM^{-1}. (D) Concentration dependence of the steady-state current. Experimental data from same axon as in (B). Dashed line is the curve for the open-state block predicted from data in (C). $K_d = 617$ μM and $n_H = 1$. Continuous line is the curve predicted by a model assuming blocking mechanisms in separate channel populations (see text). Dotted lines show the predicted curves for the two separate populations. The population containing an open-state dependent block site ($K_d = 617$ μM and $n_H = 1$) comprises 25% of the total population. The corresponding values for the population containing a state-independent block site are $K_d = 48$ μM, $n_H = 3.6$ and 75% of the total population.

The time course effect seen in Fig. 2, is more clearly illustrated in Fig. 4B. It shows the current at +50 mV (close to Na^+ equilibrium potential to minimise contaminating Na^+ current; see above) for control and two bupivacaine concentrations. The induced inactivation was found to follow a monoexponential time course. The associated time constant was found to be voltage independent (tested in the range +50 to +90 mV where the K^+ current is relatively uncontaminated by Na current). Values for the inverse time constants, reflecting the rate of inactivation, and corresponding steady-state currents for a 50-ms test pulse to 50 mV, are plotted against bupivacaine concentration in Fig. 4C and D. (For lower concentrations than 50 μM bupivacaine the rate of inactivation was too small to yield reliable time constants and steady-state values. For the 33 μM value in Fig. 4C we used direct measurements of the current at the end of the pulse.) The induced inactivation suggest an open-state dependent block. To quantitatively explore this effect we used the following model:

$$\mathrm{C} \quad \rightleftharpoons \quad \mathrm{O} \quad \underset{\lambda}{\overset{\kappa\, c_{\mathrm{bup}}}{\rightleftharpoons}} \quad \mathrm{OB} \qquad (5)$$

C, O, and OB denote closed, opened and blocked states, respectively, and κ and λ binding and unbinding rate constants. Assuming a fast opening rate (compared to the blocking rate), this model predicts a linear relation between the inverse of the time constant and bupivacaine concentration according to

$$1/\tau = \kappa\, c_{\mathrm{bup}} + \lambda. \qquad (6)$$

Fitting this equation to the data in Fig. 4C yields $\lambda = 0.08$ ms^{-1} and $\kappa = 0.13$ ms^{-1} mM^{-1}. These values predict a K_d value (λ/κ) of 617 μM at steady state. The dose–response curve calculated on these values (dashed line) and experimental values are compared in Fig. 4D.

The discrepancy between measured (half value about 60 μM) and predicted data supports the conclusion from the open probability curve experiments (Fig. 4A) of a dominant state independent block. The mean K_d for three axons was 550 ± 71 μM. For simplicity the model discussed (Eq. (5)) assumes 1:1 binding stoichiometry. Models assuming higher binding stoichiometries and different cooperativities between the steps were also tested. These more complex models did not markedly improve the fit between experimental and predicted rate constants, thus validating the simplifying assumption.

From the above, we thus conclude that the bupivacaine block of nodal K^+ channels cannot be fully explained by an open-state block. This was further supported by the result of an analysis of the bupivacaine induced inactivation time course. If an open state block is assumed to fully explain the effect on the K^+ channels, and if the rate of the induced inactivation is much slower than the activation (10-fold or more which was the case for concentrations up to 1 mM), then the bupivacaine affected current, extrapolated back to time zero, should be approximately equal to the non-affected steady-state current. This was not the case in any of the five more extensively analysed axon (see Fig. 4B). We thus conclude that the bupivacaine block of nodal K^+ channels can be explained in terms of two independent mechanisms, mediated by separate sites of action; one state independent and one open-state dependent. The data further suggest that the two tentative sites are located on channels belonging to two separate populations. This statement is based on results from fitting procedures of the type shown in Fig. 4D. It shows a dose–response curve (continuous line) defined as the sum of the dose–response curves for the state-independent and the state-dependent blocking, respectively (dotted curves) fitted to experimental data from the same axon discussed above. This dose–response curve thus represents the expected curve if the two binding sites are assumed to belong to separate channel populations. For the fitting procedure K_d and n_H values for the open-state block were assumed to be 617 μM and 1, respectively (i.e., the same as those of the dashed line). The resulting values for the state-independent block were $K_d = 70$ μM and $n_H = 2.0$, respectively. The relative size of the channel population blocked state-independently was 75% of the total population. Mean K_d and n_H for the state independent block of three axons were 59 ± 11 μM and 2.8 ± 0.9.

In conclusion, the bupivacaine effect on the nodal K^+ channels can be explained by two mechanisms with independent binding sites. The findings further suggest that the two tentative sites are located on separate channel populations; one site being high-affinity (59 μM) and state-independent and the other low-affinity and open-state dependent (550 μM). The high-affinity site shows higher than 1:1 binding stoichiometry, suggesting that at least two bupivacaine molecules are required to block the channel at this site. Considering the affinity and the stoichiometry, the high-affinity site shows similarities to the Na^+ channel site.

4. Discussion

The main conclusion from the present work is that the anaesthetic action of bupivacaine in myelinated axons is primarily due to inhibition of the Na^+ channels and not to a depolarisation due to effects on the leak current as suggested by Bräu et al. (1995). The inhibition of Na^+ channels was found to be caused by a combination of a reduced maximum open probability and a shift of the Na^+ steady-state inactivation curve. This was tentatively explained by a single binding-site model. The effect on K^+ channels was more complex. It was explained by a two-site binding model. The mechanistic implications of these hypotheses will be explored below. First, however, possible reasons for the lack of leak current effect will be outlined and discussed.

4.1. Reasons for experimental discrepancies

The reason for the discrepancy between the present negative results on the resting potential effects and the positive results reported by Bräu et al. (1995) is not clear. One possible explanation is that the reported flickering channels in the present study were inaccessible for bupivacaine in the external solution due to their location in the paranodal region. This implies, however, that a possible flickering channel effect is clinically irrelevant. Another possible reason for the discrepancy is that the present results are obscured by an extraaxonal current under the myelin sheath. This explanation can, however, be excluded. An extraaxonal current was first inferred by Dodge and Frankenhaeuser (1958), and has recently attracted renewed interest (see the work of Ritchie (1995)). The existence of such a current would mean that the presently measured leak current comprises both a nodal (and paranodal) transmembrane current and a longitudinal extraaxonal current. Consequently bupivacaine effects on the nodal component will be partially masked by the unaffected extraaxonal component. However, as shown by Dodge and Frankenhaeuser (1958), the extra-axonal current is negligible in axons cut at full internodal length. We found no effect of 6 mM bupivacaine on the leak current in such axons, suggesting that bupivacaine does not affect the transmembrane leak current in this preparation. The main effect must consequently be on Na^+ and K^+ channels.

4.2. Molecular aspects of the binding sites

4.2.1. Na^+ channels

The found inhibition of the Na^+ channels was characterised by a decrease of maximum open probability and a

shift of the steady-state inactivation curve. Such a dual (shift and scaling) effect of bupivacaine on Na^+ channels has also been reported for cardiac and GH_3 cells (Clarkson and Hondeghem, 1985; Wang and Wang, 1992; Valenzuela et al., 1995b). The size of the open probability and the shift values reported are close to those of the present investigation. An additional open-state dependent block has been observed in cardiac Na^+ channels (Valenzuela et al., 1995b). In batrachotoxin-treated Na^+ channels bupivacaine almost exclusively causes such an open-state block (Wang and Wang, 1994). The stoichiometry of the binding kinetics in the present investigation was systematically slightly higher than 1:1, suggesting that at least two molecules bound to the channel are necessary for block. This finding deviates from the 1:1 stoichiometry reported in earlier studies of bupivacaine action on Na^+ channels (Clarkson and Hondeghem, 1985; Chernoff, 1990; Wang and Wang, 1992; Valenzuela et al., 1995b), and in studies of other local anaesthetics (Århem and Frankenhaeuser, 1974). (An exception is benzocaine binding to batrachotoxin treated Na^+ channels at positive potentials which shows 2:1 stoichiometry, Wang and Wang, 1994).

A simple modulated receptor model (Eq. (3)) was presented to explain the findings. The essence of the model is that bupivacaine molecules (at least two) bind to a single site in closed or open configuration, shifting the equilibrium state of the channel towards the inactivated state. In principle, there are several models that can explain these findings (e.g., Bean et al., 1983). However, the present model was constructed to comply with current views on the Na^+ channel structure and the molecular action of local anaesthetics (e.g., Patton et al., 1992; Zamponi and French, 1994). Assuming that the intracellular linker between the third and fourth domain of the channel forms an inactivation 'lid' that binds to a hydrophobic pocket in the internal mouth of the pore (see the works of Patton et al. (1992) and Zamponi and French (1994)), bupivacaine can be assumed to bind to the hydrophobic pocket, thereby increasing the probability of the linker to bind to its site. This mechanistic scenario implies that the access of bupivacaine to bind to its site is limited to the closed and open states as assumed in the model. It is not uninteresting that the present model is compatible with the results of a recent study of the action of dibucaine on Na^+ channels (Kuroda et al., 1996). This study suggests that the increased inactivation is caused by two π-stacked dibucaine molecules bound to the intracellular hydrophobic site, thereby increasing the binding affinity of the site to the inactivating lid.

4.2.2. K^+ channels

For the effect on the K^+ channels a model was suggested that assumed two independent mechanisms mediated via two separate binding sites: one low-affinity open-state dependent site and one high-affinity state independent site. The results further suggested that the two tentative binding sites are located on separate channel populations, the population with the high-affinity site comprising about 75% of the total population. How do these tentative populations relate to the three different K^+ channel populations reported for the nodal region of *X. laevis* axons? Two of these populations show fast activation kinetics (f_1 and f_2), one shows slow (s) (Bräu et al., 1990). The results suggest that the high-affinity site population may be identical with the f_1 channel population and the low-affinity site population with the f_2 population. The reason is that the relatively fast time scale used in the present investigation excludes the s population from the discussion, and that the high-affinity site is affected at potentials where f_1 channels are activated but not f_2 (below -50 mV). The differential effect by bupivacaine on two channel populations with different affinities and different activation ranges may seem incompatible with the observed general decrease of the open probability curve as shown in Fig. 4A. However, this is not the case. The existence of a low-affinity population (activated at more positive potentials) would tend to shift the open probability curve to the right when bupivacaine is applied, while the open-state binding would tend to shift the curve to the left.

In studies of bupivacaine on human Kv1.5 channels Valenzuela et al. (1995a) concluded that the effects could be fully explained by bupivacaine binding to an open-state dependent site. They found no evidence for a second binding site. As the f_1 channel of the *Xenopus* myelinated axon of kinetic and pharmacological reasons most likely is of the Kv1.1 type (Elinder and Århem, 1998), and as there were reasons to believe that this channel did not contain an open-state dependent site, the findings of Valenzuela et al. (1995a) suggest functionally essential internal (or external) mouth structure differences between Kv1.1 and Kv1.5 channels. Preliminary experiments in collaboration with Dr. Michael Medeja (Institut für Physiologie, Münster, Germany) show that bupivacaine mainly causes a state independent block of Kv1.1 channels expressed in *Xenopus* oocytes, thus supporting the view presented above.

4.3. Remark on the differential blockade

Important clinical properties of bupivacaine are a relatively high potency and a capacity to block sensory and motor fibres differently (Covino, 1986). For example, bupivacaine is widely used extradurally for both surgical and obstetric procedures and relief pain after operations as a result of its minimal blockade of motor neurones when providing adequate sensory analgesia. The results of the present investigation are fully compatible with the higher potency of bupivacaine compared to other local anaesthetics. This is reflected in the low K_d value for bupivacaine (44 μM) compared to corresponding values for less potent local anaesthetics such as lidocaine, procaine and benzocaine (1, 1.5 and 3.0 mM, respectively; Århem and Frankenhaeuser, 1974).

The present results are, however, not compatible with the mechanism for the differential blockade proposed by Bräu et al. (1995). This mechanism was based on the assumption of relatively more bupivacaine sensitive flickering channels in thin pain fibres. Nevertheless, a differential blockade of thin pain fibres is easily conceived within the frames of the present findings. For instance, thin fibres are more sensitive to internal ion concentration disturbances than thick ones, and a bupivacaine induced shift of the inactivation curve is therefore likely to have more profound consequences for thin than for thick fibres. The differential effect on two K^+ channel populations may also be relevant for the issue. If the suggested identification of the high-affinity/low-affinity populations with the f_1/f_2 populations is valid, a differential bupivacaine effect on sensory and motor axons is predicted (f_1 channels dominate in motor axons and f_2 channels in sensory axons).

Acknowledgements

This work was supported by grants from the Swedish Medical Research Council (Project No. 6552), Karolinska Institutet, Hjärnfonden and the Swedish Society of Medicine. We thank Dr. Peter Larsson for valuable comments.

Appendix A. The relation between shift values and factor *A* in the bupivacaine block model for the Na^+ channel (Eq. (3))

For the quantification of A in the model described by Eq. (3) an analytical derivation of the relation between A and the shift value ($\Delta V_{1/2}$) is given below. The fraction of channels available for opening $f_C(V)$ at a concentration c_{bup} and at potential V is

$$f_C(V) = C/(C + I + CB + IB). \quad (A1)$$

From Eqs. (1)–(3) we obtain the following expressions for the inactivated (I), the bound closed (CB) and the bound inactivated (IB) states.

$$I = C \exp\left(-(V - V_{1/2})/s\right) \quad (A2)$$

$$CB = C\left(c_{bup}/K_d\right)^{n_H} \quad (A3)$$

$$IB = A\,C\left(c_{bup}/K_d\right)^{n_H} \exp\left(-(V - V_{1/2})/s\right) \quad (A4)$$

The midpoint potential $V_{1/2}$ (potential for 50% of max value) and slope s refer to the inactivation curve in control solution. From Eq. (A1)–Eq. (A4) we get

$$f_C(V) = 1/\left(1 + \exp\left(-(V - V_{1/2})/s\right) + \left(c_{bup}/K_d\right)^{n_H} + A\left(c_{bup}/K_d\right)^{n_H} \exp\left(-(V - V_{1/2})/s\right)\right). \quad (A5)$$

The fraction of channels that can be opened at the midpoint potential $V = V_{1/2} + \Delta V$ at concentration c_{bup} is 0.5 I_{max}. From Eq. (2) we thus obtain

$$f_C(V) = 0.5/\left(1 + \left(c_{bup}/K_d\right)^{n_H}\right). \quad (A6)$$

Applying this expression to Eq. (A5) we get

$$\Delta V = s \ln\left[\left(1 + A\left(c_{bup}/K_d\right)^{n_H}\right)\left(1 + \left(c_{bup}K_d\right)^{n_H}\right)\right] \quad (A7)$$

which will be used to determine the factor A.

References

Århem, P., Frankenhaeuser, B., 1974. Local anesthetics: effects on permeability properties of nodal membrane in myelinated nerve axons from *Xenopus*. Potential clamp experiments. Acta Physiol. Scand. 91, 11–21.

Århem, P., Frankenhaeuser, B., Moore, L.E., 1973. Ionic currents at resting potential in nerve axons from *Xenopus laevis*: potential clamp experiments. Acta Physiol. Scand. 88, 446–454.

Bean, B.P., Cohen, C.J., Tsien, R.W., 1983. Lidocaine block of cardiac sodium channels. J. Gen. Physiol. 81, 613–642.

Bräu, M.E., Dreyer, F., Jonas, P., Repp, H., Vogel, W., 1990. A K^+ channel in *Xenopus* nerve fibres selectively blocked by bee and snake toxins: binding and voltage-clamp experiments. J. Physiol. 420, 365–385.

Bräu, M.E., Nau, C., Hempelmann, G., Vogel, W., 1995. Local anaesthetics potently block a potential insensitive potassium channel in myelinated nerve. J. Gen. Physiol. 105, 485–505.

Butterworth, J.F. IV, Strichartz, G.R., 1990. Molecular mechanisms of local anesthesia: a review. Anesthesiology 4, 711–734.

Chernoff, D.M., 1990. Kinetic analysis of phasic inhibition of neuronal sodium currents by lidocaine and bupivacaine. Biophys. J. 58, 53–68.

Clarkson, C.W., Hondeghem, L.M., 1985. Mechanism for bupivacaine depression of cardiac conduction: fast block of sodium channels during the action potential with slow recovery from block during diastole. Anesthesiology 62, 396–405.

Covino, B.G., 1986. Pharmacology of local anaesthetic agents. Br. J. Anaesthesiol. 58, 701–716.

Dodge, F., Frankenhaeuser, B., 1958. Membrane currents in isolated frog nerve axon under voltage clamp conditions. J. Physiol. 143, 76–90.

Elinder, F., Århem, P., 1998. The functional surface charge density of a fast K channel in the myelinated axon of *Xenopus laevis*. J. Membr. Biol. 165, 175–181.

Frankenhaeuser, B., 1957. A method for recording resting and action potentials in the isolated myelinated nerve fibre of the frog. J. Physiol. 135, 550–559.

Haydon, D.A., Elliot, J.K., Hendry, B.M., 1984. Effects of anaesthetics on the squid giant axon. Curr. Top. Membr. Transp. 22, 445–482.

Hille, B., 1977. Local anesthetics: hydrophilic and hydrophobic pathways for the drug–receptor reaction. J. Gen. Physiol. 69, 497–575.

Hille, B., 1992. Ionic Channels of Excitable Membranes. Sinauer, Sunderland, MA, 612 pp.

Hondeghem, L.M., Katzung, B.G., 1977. Time and voltage dependent interactions of antiarrhythmic drugs with cardiac sodium channels. Biochim. Biophys. Acta 472, 373–398.

Koh, D.S., Jonas, P., Bräu, M.E., Vogel, W., 1992. A TEA-insensitive flickering potassium channel active around the resting potential in myelinated nerve. J. Membr. Biol. 130, 149–162.

Kuroda, Y., Ogawa, M., Nasu, H., Terashima, M., Kasahara, M., Kiyama, Y., Wakita, M., Fujiwara, Y., Fujii, N., Nakagawa, T., 1996. Locations of local anesthetic dibucaine in model membranes and the interaction between dibucaine and a Na channel inactivation gate

peptide as studied by ^{2}H and ^{1}H NMR spectroscopies. Biophys. J. 71, 1191–1207.

Patton, D.E., West, J.W., Catterall, W.A., Goldin, A.L., 1992. Amino acid residues required for fast Na^{+}-channel inactivation: charge neutralisations and deletions in the III–IV linker. Proc. Natl. Acad. Sci. USA 89, 10905–10909.

Ritchie, J.M., 1995. Physiology of axons. In: Waxman, S.G., Kocsis, J.F., Stys, P.K. (Eds.), The Axon. Oxford University Press, Oxford.

Valenzuela, C., Delpon, E., Tamkun, M.M., Tamargop, J., Snyders, D.J., 1995a. Stereoselective block of a human cardiac potassium channel (Kv1.5) by bupivacaine enantiomers. Biophys. J. 69, 418–427.

Valenzuela, C., Snyders, D.J., Bennett, P.B., Tamargo, J., Hondeghem, L.M., 1995b. Stereoselective block of cardiac sodium channels by bupivacaine in guinea pig ventricular myocytes. Circulation 92, 3014–3024.

Wang, G.K., Wang, S.Y., 1992. Altered stereoselectivity of cocaine and bupivacaine isomers in normal and batrachotoxin modified Na^{+} channels. J. Gen. Physiol. 100, 1003–1020.

Wang, G.K., Wang, S.Y., 1994. Binding of benzocaine in batrachotoxin modified Na^{+} channels: state-dependent interactions. J. Gen. Physiol. 103, 501–518.

Zamponi, G.W., French, R.J., 1994. Amine blockers of the cytoplasmic mouth of sodium channels: a small structural change can abolish voltage dependence. Biophys. J. 67, 1015–1027.